

## Imaging of Saddle Point Electron Emission in Slow $p$ -He Collisions

R. Dörner,<sup>1,2,\*</sup> H. Khemliche,<sup>3</sup> M. H. Prior,<sup>3</sup> C. L. Cocke,<sup>2</sup> J. A. Gary,<sup>4</sup> R. E. Olson,<sup>4</sup> V. Mergel,<sup>1</sup>  
J. Ullrich,<sup>5</sup> and H. Schmidt-Böcking<sup>1</sup>

<sup>1</sup>*Institut für Kernphysik, Universität Frankfurt, August Euler Strasse 6, D60486 Frankfurt, Germany*

<sup>2</sup>*Department of Physics, Kansas State University, Manhattan, Kansas 66506*

<sup>3</sup>*LBNL, Berkeley, California 94720*

<sup>4</sup>*University of Missouri, Rolla, Missouri 65401*

<sup>5</sup>*Gesellschaft für Schwerionen Forschung, D64291 Darmstadt, Germany*

(Received 6 May 1996)

The two-dimensional velocity distribution of electrons emitted in 5–15 keV  $p$ -He collisions has been measured for completely determined motion of the nuclei, that is, as a function of the impact parameter and in a well defined scattering plane. The electrons are emitted preferentially in the scattering plane and in the forward direction. The velocity distributions show sharp structures that vary strongly with impact parameter and projectile velocity. The results are compared to classical trajectory calculations. [S0031-9007(96)01614-6]

PACS numbers: 34.50.Fa

In ion-atom collisions, where the velocity of the projectile is much slower than the classical Bohr velocity of the target electrons, the dominant process which ionizes the target is electron capture to bound states of the projectile. Compared to this capture transition, the emission of an electron into the continuum is extremely unlikely [1]. While in a fast ion collision direct ionization by light projectiles is rather well understood, there has been much discussion of which mechanism promotes electrons into the continuum in slow collisions.

On the grounds of classical mechanics, Olson [2] suggested a “saddle point mechanism.” The potential between the projectile and the residual target ion has a point (the saddle point) where no force acts on an electron moving between them. As the projectile and target separate, the potential rises and hence electrons traveling with the velocity of this saddle could be “left stranded” in the continuum between the target and projectile [2]. The relative importance of this mechanism has been discussed within the theoretical framework of classical mechanics [2–4] as well as in various quantum mechanical approaches [5–12]. Many experimental studies have sought evidence for it in ionization [3,13–16] and excitation [17,18]. Recently Piekma and co-workers [19] measured the velocity distribution of electrons emitted in 1–6 keV  $p$ -H collisions integrated over all emission angles and found a maximum of the cross section at the velocity of the saddle point. Kravis and co-workers [20] obtained two-dimensional images of the longitudinal and transverse velocity of the continuum electrons, using a technique similar to that used here, but without impact parameter determination, for a wide range of impact velocities of  $p$  and  $C^{6+}$  projectiles. Only for proton impact below 1 a.u. (atomic unit velocity) did they find most of the electrons in the saddle point region. Within the hidden crossing theory [9] ionization at these slow velocities has been explained as a multistep promotion process in

the quasimolecule formed during the collision, and characteristic electron velocity distributions in the scattering plane have been predicted for a quantum mechanical analog of the classical saddle point mechanism [11,12].

In this Letter we present an experimental study of 5–15 keV  $p$ -He collisions, which, for the first time give two-dimensional images of the square of the final state electron wave function in velocity space *with simultaneous determination of the impact parameter and the orientation of the scattering plane*. We used cold target recoil ion momentum spectroscopy [21–24] to determine the nuclear motion (i.e., impact parameter and scattering plane) by detecting the three-dimensional momentum vector of the target ion in coincidence with two momentum components of the emitted electron.

The key to both, the electron and the recoil ion momentum measurement is a well localized and internally cold He gas target provided by a supersonic gas jet [21–23,25]. The interaction volume, defined by the jet and beam diameter is about 0.5 mm<sup>3</sup>. By a combination of weak (17 V/cm) extraction and focusing fields and a drift space, the recoil ions are projected onto a position sensitive channel plate detector. A second similar detector for electrons is mounted 22 mm from the interaction region opposite the ion detector. The electric field projects the electrons onto this electron detector. From the position and the time of flight, measured by a coincidence with the electron, one obtains the charge state and the three momentum components of the ion. Since the electron time of flight was not measured, it was assumed constant in order to calculate two momentum components from the electron detector position signal. An electron velocity of 0.1 a.u. directed parallel or antiparallel to the field yields about a 6% change in the electron time of flight and thus a similar error in momentum components transverse to the field calculated from the electron position. Our results presented below show that the electron momenta

perpendicular to the scattering plane are, in most cases, below 0.1 a.u. This technique of electron velocity space mapping by projection from a localized source volume onto a position sensitive detector allows a  $4\pi$  detection efficiency for all electrons even at 0 eV continuum energy, with a resolution  $<40$  meV at 0 eV. Similar techniques have previously been used by several groups [20,24,25].

In the off-line analysis we create electron position distributions gated on selected transverse recoil ion momenta and azimuthal angles of the ion. By choosing events for different azimuthal angles in the detector frame we can effectively rotate the collision plane (defined by the beam axis and the recoil ion momentum vector) with respect to our electron detector.

Figure 1(a) shows the transverse momentum distribution of the ions  $d\sigma/dp_{\perp\text{He}^+}$  for ionizing collisions. From momentum conservation the transverse momenta of the electron, the ion, and the projectile must sum to zero.

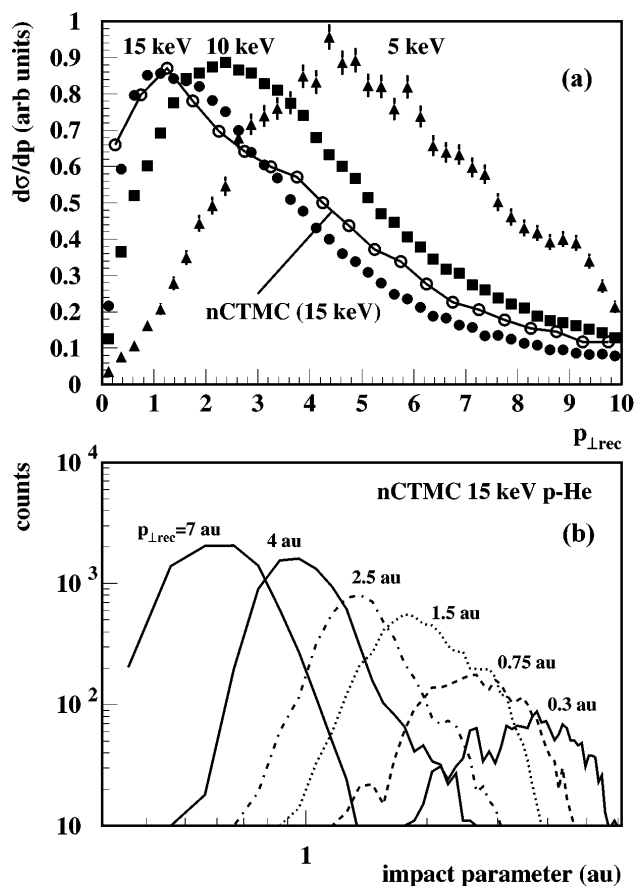


FIG. 1. (a) Transverse momentum distribution of the recoil ions in ionizing collisions for 5, 10, and 15 keV  $p$ -He. Open circles with full line: CTMC calculation for 15 keV. The experiment is not on an absolute scale. (b) Relation between recoil ion transverse momentum and impact parameter for 15 keV from CTMC calculation. The lines show the distribution of impact parameters which contribute to the transverse momentum indicated in the figure.

However, as we show below, the typical transverse momenta of the electrons in these slow collisions are below 0.3 a.u. and thus the  $p_{\perp\text{He}^+}$  reflects almost perfectly the transverse momentum of the projectile, and the projectile scattering angle ( $\vartheta_{\text{pro}} \approx p_{\perp\text{He}^+}/p_0$ , where  $p_0$  is the longitudinal momentum of the projectile). For 15 keV proton energy we performed classical trajectory monte carlo (CTMC) calculations which are found to be in good agreement with the data. In order to discuss our data in an impact parameter picture, we show the relation between impact parameter and transverse recoil momentum  $p_{\perp\text{He}^+}$  obtained from the CTMC calculations [Fig. 1(b)]. The three-body, three-dimensional calculation method was employed with the interaction potentials the same as in Refs. [2,3]. However, because of the slowness of the collision it was deemed necessary to considerably improve upon the usual microcanonical distribution. In order to accomplish this we used a Wigner distribution of ten initial binding energies so that the quantum mechanical radial probability distribution was reproduced over 4 orders of magnitude ( $R_E = 5a_0$ ). In turn, the microcanonical electronic momentum distribution also improved, rather than degraded, when compared to the quantum mechanical one. Hence, although the trajectory of the individual particles were governed by classical mechanics, the initial electronic distributions were determined from quantum mechanics.

We summarize our experimental findings in Figs. 2(a)–2(d), which show the impact parameter dependence, and Figs. 3(a)–3(d), which show the projectile velocity dependence of the electron emission. All spectra except for Fig. 3(d) display the projection of the velocity distribution of the electrons onto the scattering plane, defined by the beam direction ( $z$ ) and the recoil ion momentum vector, for fixed  $p_{\perp\text{He}^+}$  (i.e., impact parameter). The recoil ion is directed towards negative  $v_{ex}$ , i.e., the projectile passed on the side of positive  $x$ . The units are  $v_e/v_p$  with the electron velocity  $v_e$  and the projectile velocity  $v_p$ . Therefore, target-centered electron emission would appear around the origin while electrons captured to continuum states of the projectile would be located at the second cross at ( $v_{ez}/v_p = 1$  and  $v_{ex} = 0$ ). The saddle point is located in the center between target and projectile since both ions are singly charged in the final state. Note that the cross section is displayed in Cartesian coordinates as  $d^2\sigma/dv_x dv_z$ . This presentation gives a graphic image of the square of the final state wave function and does not tend to force the cross section to zero for  $v_e \rightarrow 0$ .

For large impact parameters [ $b > 1$  a.u.,  $p_{\perp\text{He}^+} < 5$  a.u. at 15 keV; see Fig. 1(b)], which give the dominant contribution to the ionization cross section, we find nearly all electrons in a broad range around the saddle point, between target and projectile [Figs. 2(a), 2(b), and 3(a)–3(d)]. A similar picture was seen by Kravis and co-workers [20]. However, the emission exhibits a strong impact parameter dependence [Figs. 2(a)–2(d)].

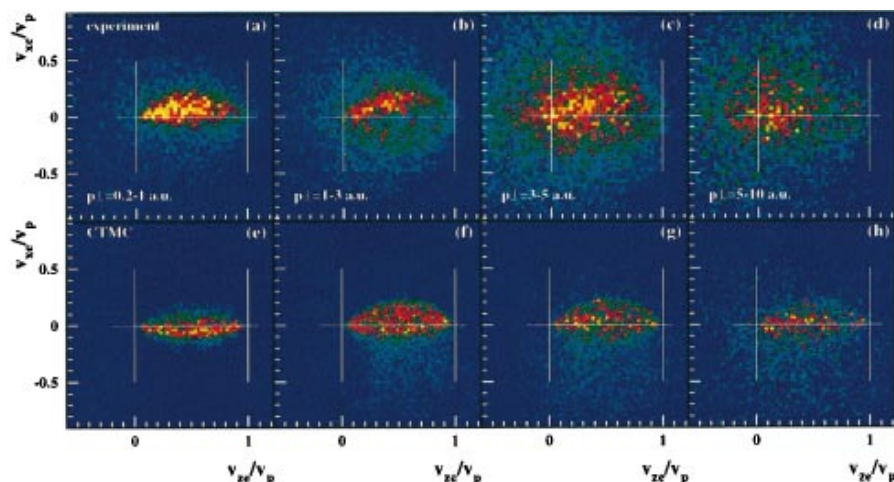


FIG. 2(color). Projection of the velocity distribution of electrons for single ionization in 15 keV  $p$ -He collisions onto the scattering plane, defined by the beam axis ( $z$ ) and the momentum of the target ion, recoiling in the  $-x$  direction. The target center is at  $(0, 0)$ , the projectile at  $(1, 0)$ , and the saddle at  $(0.5, 0)$ . (a)–(d) Experiment for different transverse momentum transfer (i.e., impact parameters), (e)–(h) CTMC.

For collisions where the projectile penetrates the target shell we find mostly target-centered electrons [Fig. 2(d)]. The experiment shows almost no projectile centered electrons, indicating that the electron capture to the continuum gives only a negligible contribution to the total ionization cross section for  $p$  impact at the collision energies discussed here.

From the comparison of Figs. 3(b) and 3(d) it can be seen that the electron emission is mainly in the scattering plane. This can be understood as a result of angular momentum transfer. The angular momentum transferred to the electronic wave function must be perpendicular to the scattering plane. The linear momentum of such states, for nonzero  $l$ , lies preferentially in the scattering plane.

At 10 keV, the in-plane emission splits into two narrow forward-directed jets of electrons [Fig. 3(b)]. This results in a minimum at the saddle point, with two maxima off the projectile axis. The relative strength of these two jets varies rapidly with impact velocity. At 5 keV the emission is preferentially opposite the scattered projectile (i.e., towards the direction of the recoiling target nucleus), while at 15 keV the emission is directed towards the scattered projectile. The details of the forward jets also vary with impact parameter, as can be seen in Figs. 2(a)–2(c).

Since the saddle point mechanism was proposed on the basis of classical mechanics, it is of great interest to see to what extent a classical calculation can reproduce the details of the process. Figures 2(e)–2(h) show that the CTMC calculation correctly predicts the emission of the electrons in the region of the saddle. It also qualitatively describes the preferential emission towards the positively charged projectile at 15 keV.

Although no detailed study of the impact parameter dependence of the electron emission pattern has been performed within the theory of hidden crossings, some

speculations are invited by our data. As discussed by Pieksma and Ovchinnikov [12] and Ovchinnikov and Macek [11] two series of transitions (T00 and T01) are expected to contribute to the saddle point mechanism. The T00 series involves no angular momentum transfer and thus leads to a  $\sigma$  state in the saddle point continuum, while the T01 series starts with a rotational coupling to the  $2p\pi$  orbital of the quasimolecule and leads to a  $\pi$  state. It is this different symmetry of  $\sigma$  and  $\pi$  states which according to the calculations yields a maximum on the saddle for the T00 and a node for the T01 series. Thus the minimum on the saddle, with two maxima off axis, observed at 10 keV, may be the first direct experimental observation of characteristics of the T01 series. However, the transition amplitudes of all series have to be added coherently [27]. The relative phase between these amplitudes varies with impact velocity [12]. Therefore one could speculate that the change in phase between the T01 and T00 from 5 to 15 keV leads to the observed change in weight of the two jets in the electron velocity distribution. To prove this hypothesis a detailed study including the phase as well as the impact-parameter dependence of all relevant series of molecular transitions is highly desirable.

In conclusion we have obtained images of the square of the final state wave function of the continuum electron for a fully determined motion of the nuclei. At 15 keV a CTMC calculation could qualitatively reproduce the observed emission patterns. We find a strong impact-parameter dependence of the electron emission. At small impact parameters the emission is target centered while at larger distances, which contribute most to the total cross section, the electrons are found in the region of the saddle point. These forward electrons are emitted in two jets oriented in the scattering plane in the forward direction and off the projectile axis. The relative strength of these

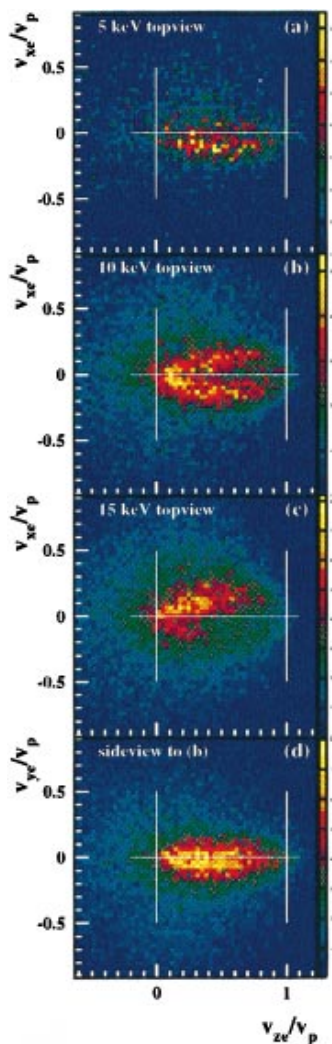


FIG. 3(color). (a)–(c) Similar to Fig. 2, but for 5, 10, 15 keV impact energy. The transverse momentum transfer is 1–5 a.u. at 10 keV. For other energies these values are scale by  $1/v_{\text{pro}}$  in order to sample approximately the same range of impact parameters. (d) Sideview to (b), i.e., projection onto the  $x, y$  plane, which is perpendicular to the scattering plane.

two jets strongly varies with impact velocity. The most probable direction of the emission switches from the side on which the projectile passes at 15 keV to the opposite side at 5 keV. The surprising richness of the distributions provides a challenge as well as a profound test ground for future theoretical work on electron emission at slow impact velocities.

This work was supported by the Division of Chemical Sciences, Office of Basic Energy Sciences, Office of Energy Research, U.S. Department of Energy, and by

NSF-Int 9112815, the Max Planck Forschungspreis of the Alexander von Humboldt Stiftung, the DFG and BMBF, the Graduiertenförderung des Landes Hessen and the Willkomm Foundation. One of us (R.D.) gratefully acknowledges support from the Alexander von Humboldt Foundation and (V.M.) of the Studienstiftung des deutschen Volkes. We thank S. Kravis, J. Macek, S. Ovchinnikov, C.D. Lin, Y.D. Wang, M. Pieksma, and G. von Oppen for very helpful discussions.

\*Electronic address: doerner@ikf007.ikf.physik.uni-frankfurt.de

- [1] W. Wu *et al.*, Phys. Rev. Lett. **75**, 1054 (1995).
- [2] R.E. Olson, Phys. Rev. A **27**, 1871 (1983); **33**, 4397 (1986).
- [3] R.E. Olson *et al.*, Phys. Rev. Lett. **59**, 36 (1987).
- [4] G. Bandarage and R. Parson, Phys. Rev. A **41**, 5878 (1990).
- [5] T.G. Winter and C.D. Lin, Phys. Rev. A **29**, 3071 (1984).
- [6] T.G. Winter, Phys. Rev. A **37**, 4656 (1988).
- [7] A. Barany and S. Ovchinnikov, Phys. Scr. **T46**, 243 (1993).
- [8] R.K. Janev *et al.*, Phys. Rev. A **49**, R645 (1994).
- [9] E.A. Solovov, Phys. Rev. A **42**, 1331 (1990).
- [10] J.H. Macek and S.Yu. Ovchinnikov, Phys. Rev. A **50**, 468 (1994).
- [11] S.Yu. Ovchinnikov and J. Macek, Phys. Rev. Lett. **75**, 2474 (1995).
- [12] M. Pieksma and S.Yu. Ovchinnikov, J. Phys. B **27**, 4573 (1994).
- [13] W. Meckbach *et al.*, Phys. Rev. Lett. **57**, 1587 (1986); J. Phys. B **24**, 3763 (1991).
- [14] T.J. Gay *et al.*, J. Phys. **23**, L823 (1990).
- [15] V.D. Irby *et al.*, Phys. Rev. A **47**, 2957 (1993).
- [16] R. DuBois, Phys. Rev. A **48**, 1123 (1993).
- [17] S. Büttrich and G. von Oppen, Phys. Rev. Lett. **71**, 3778 (1993).
- [18] G. v. Oppen, Europhys. Lett. **27**, 279 (1994).
- [19] M. Pieksma *et al.*, Phys. Rev. Lett. **73**, 46 (1994).
- [20] S.D. Kravis *et al.*, Phys. Rev. A **54**, 1394 (1996).
- [21] R. Dörner *et al.*, Phys. Rev. Lett. **72**, 3166 (1994).
- [22] V. Mergel *et al.*, Phys. Rev. Lett. **74**, 2200 (1995).
- [23] J. Ullrich *et al.*, Comments At. Mol. Phys. **30**, 285 (1994).
- [24] R. Moshhammer *et al.*, Phys. Rev. Lett. **73**, 3371 (1994).
- [25] R. Moshhammer *et al.*, Nucl. Instrum. Methods Phys. Res., Sect. B **108**, 425 (1996).
- [26] H. Helm *et al.*, Phys. Rev. Lett. **70**, 3221 (1993).
- [27] We thank J. Macek and S.Yu. Ovchinnikov for pointing out that these amplitudes must be added coherently and that their relative phases should be velocity dependent.